




# Alginate-Bentonite Clay Composite Porous Sorbents for Cu(II) and Zn(II) Removal from Water

Christine Hood · Erica Pensini 

Received: 27 August 2021 / Accepted: 29 March 2022 / Published online: 6 April 2022  
© The Author(s), under exclusive licence to Springer Nature Switzerland AG 2022

**Abstract** High concentrations of heavy metals in groundwater are harmful to humans and ecological receptors. This study uses natural alginate-based sorbents for the removal of heavy metals (e.g., copper, zinc, iron, and nickel) from water. The effectiveness of alginate-based sorbents was enhanced by adding calcium bentonite clay and by tuning the porosity of the sorbents. Controlled porosity was obtained by an acid base reaction, using sodium carbonate and acetic acid. The maximum sorption capacity of alginate-based sorbents was  $127.9 \pm 0.6$  mg/g and  $148.1 \pm 0.2$  mg/g for Cu(II) and Zn(II), respectively. The sorption of Zn(II) onto the sorbents followed pseudo first-order kinetics ( $k_1 = 9.71 \times 10^{-3}$ ), indicating that the rate limiting step was the diffusion of Zn(II) into the sorbents. In contrast, the sorption of Cu(II) onto the sorbents followed pseudo second-order kinetics ( $k_2 = 5.80 \times 10^{-5}$ ), indicating that the rate limiting step was chemisorption of Cu(II) into the sorbents. Optical microscopy images of the sorbent cross-section showed pore shrinking following sorption of either Zn(II) or Cu(II), due to crosslinking of alginate by these metal ions. Cu(II) diffusion into the sorbents was further demonstrated by blue discoloration (as shown by images of their cross sections) and by attenuated total reflection-Fourier transform

infrared spectroscopy (ATR-FTIR). Intraparticle diffusion plots of both Zn(II) and Cu(II) showed that the sorption process begins with surface adsorption and is followed by the rate controlled step of intraparticle diffusion. Alginate-based sorbents could also be used to effectively remove other divalent ions (e.g., Ni(II)), whereas removal of trivalent ions (e.g., Fe(III)) was less effective.

## Highlights

Alginate-clay composites remove Zn(II) and Cu(II) from water.

Porous sorbents are more effective than non-porous sorbents.

Calcium bentonite clay enhances Zn(II) and Cu(II) sorption.

Sorption kinetics are first order for Zn(II) and second order for Cu(II).

The rate controlling step for Zn(II) and Cu(II) sorption is intraparticle diffusion.

**Keywords** Copper · Zinc · Water Purification · Sorbent · Alginate

## 1 Introduction

Industrial development has increased the consumption and mining of heavy metals, which are detrimental to human and ecological receptors when they leach

C. Hood · E. Pensini (✉)  
School of Engineering, University of Guelph, 50 Stone  
Road East, Guelph, ON N1G 2W1, Canada  
e-mail: epensini@uoguelph.ca

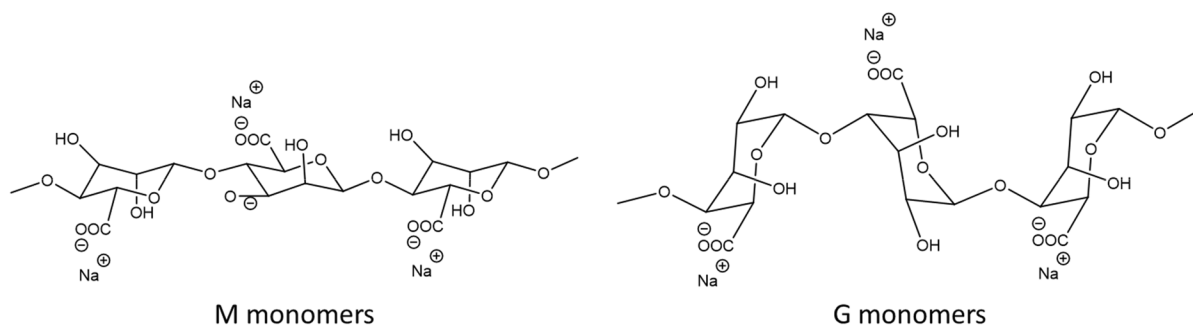
into the environment (Joseph et al., 2019; Kayranli et al., 2021). Examples of heavy metals are copper and zinc, which are toxic at high concentrations (Burton et al., 2005; Flemming & Trevors, 1989). Various approaches have been developed to remove toxic metals from either groundwater (Pensini et al., 2021; Telepanich et al., 2021) or surface waters (Foong et al., 2020; Hosseini et al., 2020; H. Wu et al., 2019). Electrodeposition can effectively purify water while also separating the metals into their pure form (which has commercial value) (Karatutlu et al., 2018). Nonetheless, the treatment can be time consuming and costly (Karatutlu et al., 2018). This approach has been specifically proposed for the removal of copper and zinc from mine tailing (Ortiz-Soto et al., 2019) and contaminated soil (Rezaee et al., 2017). Ion exchange resins can be used to selectively remove harmful metals and release more benign ions in their place (Hosseini et al., 2020). Ion exchange resins have been used for the treatment of mining tailings (Botelho Junior et al., 2019) and industrial wastewater (Choi et al., 2020). They have also been used to remove zinc from river water and wastewater (Murray & Örmeci, 2019). While ion exchange resins are effective at neutral pH, these materials have low pH and thermal resistance, as well as high initial and maintenance costs (Hosseini et al., 2020). Membrane filtration has also been proposed to treat water contaminated by heavy metals (Foong et al., 2020), such as copper and zinc in industrial wastewater and acid mine drainage (Borbély & Nagy, 2009; Menzel et al., 2021). This method produces limited solid waste and uses limited amounts of chemicals, although membrane fouling and the high cost of maintenance are a disadvantage (Foong et al., 2020). Chemical treatments that precipitate toxic metals out of solution may also be used, and they have been applied for the removal of copper and zinc from water (L. P. Wang & Chen, 2019). These treatments are fairly inexpensive and easy to perform, although the resulting sludge formed in these treatments may pose environmental issues (H. Wu et al., 2019).

Sorption is a promising technique for heavy metal removal as it produces few secondary pollutants, is simple to perform, and can be highly effective (Anirudhan et al., 2012; Batmaz et al., 2014). Sorbents in general and bio-based sorbents in particular have been proposed for the removal of either zinc (Kayranli et al., 2021) or copper (Dos Santos et al., 2011; Krstić et al., 2018) from water. Bio-based materials

are particularly promising because they are abundant and biodegradable (X. Gao et al., 2019; S. Wang et al., 2018). They are a useful method for the treatment of agricultural water (Malicevic et al., 2020), and they would also be an applicable option for greenhouse pond water, where the concentrations of zinc are regulated (Maguire et al., 2018). They can also be used to treat other types of surface water and industrial water contaminated by diverse pollutants, including heavy metals (Cruz-Briano et al., 2021; Dahlan & Hafiz, 2011; P. Gao et al., 2014; Iyer et al., 2019; Ren et al., 2012; Safieh et al., 2019; Tavares et al., 2011; Q. Zhang et al., 2013).

Sodium alginate (SA) is a natural polysaccharide derived from alginic acid found in brown algae and is a byproduct of the iodine and mannitol extraction process (Lee & Mooney, 2012). SA has many uses due to its low cost, low toxicity, and gelation properties (Wee and Gombotz 1998). It is extracted from brown algae by first crushing the plant matter, then conducting alkaline extraction of the crushed material, followed by precipitation with calcium chloride, and finally reaction with sodium carbonate solution (Fiset et al., 2008). SA comprises of  $\beta$ -D-mannuronic acid (M) and  $\alpha$ -L-guluronic acid (G) monomers, as seen in Scheme 1. These monomers are arranged in homopolymeric blocks to form a linear anion copolymer (Homayouni et al., 2007). Oxygen atoms in the pyranose and carboxyl groups in SA can form stable chelates with certain metal ions and can therefore be used as binding sites for sorption (Ghimire et al., 2008). In general, calcium crosslinked alginate is selective towards divalent ions (whereas it has poor adsorption of monovalent ions) (Paudyal et al., 2013). For this reason, it would be a good material for sorbents aimed at removing divalent ions such as Cu(II) and Zn(II) from water.

Although SA has many advantageous properties for the sorption of metals, poor mechanical strength can be a problem (Ates et al., 2020; S. Wang et al., 2018). A potential strategy for obtaining cohesive alginate-based sorbents is to crosslink alginate (Malicevic et al., 2020). Crosslinking of SA can be achieved using various compounds including formaldehyde (Ghimire et al., 2008), glutaraldehyde (Liu et al., 2013), epichlorohydrin (Ghimire et al., 2008; Huo et al., 2009), and concentrated sulfuric acid (Dechojarassri et al., 2018). Environmentally benign divalent cations such as  $\text{Ca}^{2+}$  can also cross link



**Scheme 1** Molecular structure of  $\beta$ -D-mannuronic acid (M) and  $\alpha$ -L-guluronic acid (G) monomers in sodium alginate (Homayouni et al., 2007)

alginate to form a hydrogel (Bertagnolli et al., 2014; X. Gao et al., 2019; Tanaka et al., 1984). The G monomers bind with  $\text{Ca}^{2+}$ , causing the polymer chains to fold and stack upon themselves (Khalil et al., 2017). As a result, adjacent alginate chains transition from random coils to an ordered egg carton-like structure, which ultimately arranges into a mechanically robust net-like pattern (Khalil et al., 2017).

Another strategy to enhance the mechanical strength of alginate-based sorbents is to develop composite materials using various minerals, which can also enhance their sorption capacity. One study used SA and montmorillonite composite beads in order to adsorb Au(III) and found that sorption capacity was 1.49 mg/g (Mourpichai et al., 2018). Another study utilized a composite of combusted coal gangue and SA to adsorb Zn(II) and Mn(II) and found that the maximum uptake of the two metals was 77.68 and 64.29 mg/g, respectively (Mohammadi et al., 2019). Additionally, a study by Zhang et al. utilized magnetic bentonite, carboxymethyl chitosan, and sodium alginate composite hydrogel beads for Cu(II) adsorption and found that the removal rate was around 93%, with a maximum adsorption capacity of 56.79 mg/g (H. Zhang et al., 2019).

Calcium bentonite clay is known to be a successful sorbent of ions in solution (Lagaly, 1994). It is a main component of Fullers Earth, one of the earliest industrial cleaning agents used to decolorize various liquids without harsh chemicals (Hosterman & Patterson, 1992). Bentonite clay consists mostly of montmorillonite and has alternating tetrahedral and octahedral layers separated by interchangeable ions and water (Christidis et al., 2006). Calcium bentonite clay can be converted to sodium bentonite clay by

way of ion exchange (Christidis et al., 2006). A soluble sodium salt may be mixed with calcium bentonite causing the calcium ions to be ejected and replaced with sodium ions (Christidis et al., 2006). Calcium bentonite and SA would be attractive materials to obtain composite sorbents, because of their good sorbent properties and because calcium ions ejected from the clay can crosslink SA (Dechojarassri et al., 2018). Additionally, a study by Tan et al. showed that bentonite and SA composite beads sorbed more Cu(II) ions than SA beads alone (Tan & Ting, 2014). While effective, these beads were not porous, and high porosity is correlated with improved sorption capacity (Hu et al., 2020). Therefore, it would be beneficial to produce SA-bentonite sorbents using an approach that enables pore formation.

One challenge faced when using SA-based sorbents is their tendency to shrink when crosslinked and after drying, resulting in reduced sorption capacity (An et al., 2015; de Moura et al., 2005). Increasing sorbent porosity can resolve these issues and improve the rate of sorption (X. Wu et al., 2017). Previous studies used polyethylene glycol (PEG) as a pore forming agent and water to rinse it off the sorbents, although complete PEG removal proved to be difficult (Osman et al., 2005). PEG residuals in water following heavy metal sorption would be undesirable. Wheat starch has also been used for similar purposes, although its removal from the sorbents produces wastewater, which requires appropriate disposal and treatment, to avoid adverse environmental impacts (Nishimura & Sato, 1972). One study by Hu et al. utilized calcium carbonate as a pore forming agent in SA sorbent beads, which only required elution with acetic acid to remove the solid calcium carbonate (Hu et al.,

2020). The porous SA beads performed better than those without pores and had an adsorption capacity of 33.88 mg/g for Cu(II) (Hu et al., 2020). While effective, these beads were produced using freeze-drying, which may be challenging during the large-scale production of sorbents.

This study analyzed the sorption of Cu(II) and Zn(II) by SA and bentonite clay composites, obtained with a facile fabrication method. Sorbents were porous, because of the subsequent inclusion of sodium carbonate and acetic acid to SA-bentonite clay mixtures, which reacted to generate pores. Sorbents prepared with calcium carbonate and without bentonite clay were also studied, for comparison. Our porous sorbent preparation method is facile compared to methods which require freeze-drying to preserve pore structure (Hu et al., 2020). In our method, pore structure is maintained because of bentonite clay inclusion, and no drying is required before use. Moreover, SA-based sorbents with and without CaCl<sub>2</sub> crosslinking are compared, to assess the advantages and the disadvantages of different fabrication methods. While crosslinking can improve the mechanical properties of the sorbents, crosslinking with calcium can decrease the metal sorption of SA-based sorbents, because some sorption sites would be occupied by the crosslinker (X. Gao et al., 2020). While SA-based sorbents were previously proposed, this study uses a novel and facile fabrication method to produce SA and bentonite clay porous composites for the sorption of Cu(II) and Zn(II).

## 2 Materials and Methods

### 2.1 Materials

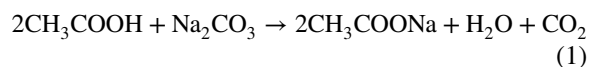
Zinc chloride (ZnCl<sub>2</sub>, Acros organics, 99%), sodium carbonate (anhydrous, powder, 99.5% pure, ACS grade), alginic acid sodium salt (90.8–106%, Spectrum), glacial acetic acid (certified ACS, 99.7% pure), calcium chloride (anhydrous, pellets 4–20 mesh, Fisher Chemical), calcium carbonate (ACS, 99% pure), zincon mono-sodium salt (quality level 100), boric acid (Fisher Bioreagent), and sodium hydroxide (ACS grade, 97%, Alfa Aesar) were purchased from Fisher Scientific (Canada). Iron chloride (Fe(III)Cl<sub>3</sub>, ACS grade) and nickel chloride (NiCl<sub>2</sub>, ACS grade) were also purchased from Fisher Scientific (Canada).

Copper chloride (99% pure), potassium cyanide (ACS reagent, > 96% pure), and cyclohexanone (ACS grade, 99% pure) were purchased from Sigma Aldrich (Canada). Calcium bentonite clay (Living Clay brand) was purchased from a local market. All reagents were used without further purification. Deionized (DI) water was used for all experiments.

### 2.2 Preparation of SA and Bentonite Clay Sorbents

Sorbents were prepared either with or without calcium bentonite clay. Sorbents with calcium bentonite clay were prepared by first combining 0.05 g or 0.1 g of clay (i.e., 1% and 2% w/w relative to the mass of SA solution) with 0.5 mL of 1 M sodium carbonate solution in a test tube and vortexing for 30 s. Next, 5 g of SA solution (1% w/w in water) was added and vortexed for 30 s. Finally, 0.5 mL of 2 M acetic acid solution was added and the mixture was vortexed for 3 s. The materials obtained were left to sit for 1 min before use. Crosslinked SA-based sorbents containing calcium bentonite clay were prepared as stated above, and then soaked in CaCl<sub>2</sub> solution (3% w/v in water) for 24 h. Crosslinked SA-based sorbents with no calcium bentonite clay were prepared by using 0.05 g CaCO<sub>3</sub> in place of the clay, and without sodium carbonate. This is because SA-based sorbents with no calcium bentonite clay or calcium carbonate were not rigid enough to be removed as one piece from their molds, before soaking in CaCl<sub>2</sub> solution.

Pores were formed by gas released in the acid base reaction of sodium (or calcium) carbonate with acetic acid, as seen in Eq. (1).



Additionally, calcium bentonite clay can release calcium ions due to ion exchange with sodium, to increase crosslinking and sorbent rigidity without the addition of CaCl<sub>2</sub> (Christidis et al., 2006).

### 2.3 Sorption Trials for Zn(II) and Cu(II)

SA-based sorbents prepared as described in Sect. 2.2 were added to 50 mL Falcon tubes with 20 mL of ZnCl<sub>2</sub> (0.1 M) or CuCl<sub>2</sub> (0.1 M) solution and shaken at 120 RPM for different time intervals (10 min, 20 min, 30 min, 1 h, 2 h, 3 h, 6 h, 12 h, or 24 h). The

pH of a 0.1 M  $\text{ZnCl}_2$  solution is 4.4, while the pH of a 0.1 M  $\text{CuCl}_2$  solution is 3. Each experiment was repeated in triplicate.

Equations (2), (3), and (4) were used to determine sorption capacity at equilibrium ( $q_e$ , mg/g) and sorption capacity at time  $t$  ( $q_t$ , mg/g) (Hu et al., 2020).

$$q_e = \frac{C_0 - C_e}{m} \times V \quad (2)$$

$$q_t = \frac{C_0 - C_t}{m} \times V \quad (3)$$

where initial and equilibrium concentrations are represented by  $C_0$  (mg/L) and  $C_e$  (mg/L), respectively; concentration at time  $t$  is  $C_t$  (mg/L);  $m$  (g) is the mass of adsorbent; and  $V$  (mL) is the volume of solution.

First- and second-order kinetic models were used to interpret the data, using Eqs. (4) and (5).

$$\text{Pseudo first order : } q_t = q_e(1 - e^{-k_1 t}) \quad (4)$$

$$\text{Pseudo second order : } q_t = \frac{k_2 q_e^2 t}{1 + (k_2 q_e t)} \quad (5)$$

where  $k_1$  and  $k_2$  are rate constants for pseudo first- and second-order sorption, respectively.

Intraparticle diffusion rates ( $k_i$ ) were obtained from the slope of the plot representing  $q_t$  vs  $t^{0.5}$ , using Eq. (6).

$$k_i = \frac{q_t}{t^{0.5}} \quad (6)$$

Sub-sets of experimental data approximately following a local linear trend were fit to separate lines using Excel, with the goal of identifying different stages of the sorption process (using a previously reported approach, (Sun & Yang, 2003; F. C. Wu et al., 2001)).

## 2.4 Spectrophotometric Determination of Zn(II), Cu(II), Fe(III), and Ni(II)

Copper solutions were analyzed before and after sorption trials using a spectrophotometer (Spectronic 200, Thermo Scientific) at a wavelength of 825 nm to determine the change in Cu(II) ion concentration. The method used was adapted from another study by Pensini et al. which analyzes changes in aqueous

copper concentration in a similar manner (Pensini et al., 2021). The wavelength of 825 nm was selected as it yielded the maximum absorbance signal. A sample of copper solution was placed in the spectrophotometer, and the maximum absorbance was recorded. The measured difference in absorbance signals between before and after sorption trials can be used to calculate the amount of Cu(II) removed from the solutions by the sorbents. The concentration of Cu(II) was calculated using calibration curves with water as the background. Iron and nickel solutions were analyzed in a similar manner, using a wavelength of 410 nm and 730 nm, respectively.

Zinc solutions were analyzed following a procedure modified from a study by D.G. Miller (Miller, 1979). Stock solutions of zinc sodium salt (1 g/L zinc sodium salt in methanol), pH buffer (8.4 g NaOH and 3.1 g  $\text{H}_3\text{BO}_3$  in 100 mL water), and KCN (10 g/L KCN in DI water) were prepared. After sorption trials, 26.8  $\mu\text{L}$  of solution was diluted in 25 mL of water. Next, 5 mL of buffer solution was added to 20 mL of diluted sample and stirred for 30 s. Then, 2 mL of KCN solution was added, followed by 3 mL of zinc sodium salt solution, stirring well between each addition. An aliquot (20 mL) of this mixture was pipetted into a separate flask, and then, 1 mL of cyclohexanone was added, stirred, and allowed to stand for 1 min. The solution without cyclohexanone was used to set the spectrophotometer for zero absorbance. The absorbance of the solution with cyclohexanone was then recorded at 625 nm. The concentration of zinc was calculated using calibration curves.

## 2.5 Optical Microscopy

An optical VHX-5000 digital microscope (Keyence, Canada) was used to observe sorbents prepared as described in Sect. 2.2, before and after sorption trials.

## 2.6 Statistical Analysis

The effect of sorbent type on copper and zinc sorption capacity at equilibrium were tested with one way analysis of variance (ANOVA) to determine if the results were statistically significant. If  $F$  values were significant ( $P < 0.05$ ), a  $t$ -test for two samples assuming unequal variances was used to probe the

significance of the difference between sorbents prepared with differing compositions.

All statistical analysis was done using Microsoft® Excel® 2016 MSO (Version 2111 Build 16.0.14701.20240) 32-bit.

## 2.7 ATR-FTIR

ATR-FTIR measurements were conducted to demonstrate copper and zinc sorption onto alginate-based sorbents. Sorbents were prepared as described in Sect. 2.2 and exposed to copper solution, to enable copper sorption over 24 h (as described in Sect. 2.3). Samples were analyzed immediately after sorption using an ATR-FTIR spectrometer (ThermoScientific Nicolet Summit FTIR spectrometer with an Everest ATR) with an accompanying IR solution software. Each spectrum represented 100 scans, with a resolution of  $2\text{ cm}^{-1}$ , in the wavenumber range of  $400\text{ to }4000\text{ cm}^{-1}$ . Measurements were conducted in triplicate.

## 3 Results and Discussion

### 3.1 Effect of Adsorbent Composition on Cu(II) Sorption at Equilibrium

Figure 1 shows sorption of Cu(II) on either SA-based sorbents (either with or without calcium bentonite clay) or calcium bentonite clay alone. The  $P$ -value of this data set was found to be  $2.58 \times 10^{-6}$ , indicating

that it is statistically significant. Sorbents obtained with SA and 1% (w/w) calcium bentonite clay (without soaking in  $\text{CaCl}_2$ ) had the highest sorption capacity ( $q_e = 127.9 \pm 0.6\text{ mg/g}$ ). Sorption of copper ions onto this sorbent was also confirmed by ATR-FTIR, which showed changes in the ATR-FTIR spectra of alginate-based sorbents following a 24-h period as seen in Fig. 2. ATR-FTIR spectra for alginate-based sorbents before and after sorption of  $\text{Cu}^{2+}$  ions showed the presence of stretching vibrations of  $-\text{OH}$  at  $\approx 3000\text{ cm}^{-1}$ . Also, the peak at  $\approx 1600\text{ cm}^{-1}$  is ascribed to the stretching of  $\text{COO}^-$  bonds. The bending vibration of  $\text{C}-\text{C}$  is represented by the absorbance peak at  $\approx 1400\text{ cm}^{-1}$ . These absorbance peaks were detected in a previous study (Mikula et al. 2019). The change in the shape of the spectrum following copper sorption indicates that functional groups in the alginate-based sorbent were involved in ion binding (Mikula et al. 2019). Additional analyses such as scanning electron microscopy–energy-dispersive X-ray spectroscopy could complement ATR-FTIR data in future research. Without 1% calcium bentonite clay, sorption capacity decreased. Nonetheless, increasing the calcium bentonite clay content from 1 to 2% decreased sorption capacity. These findings were also determined to be statistically significant by way of a  $t$ -test (wherein the results are significant if  $t$  statistic  $< t$  critical). In the case of sorbents obtained with SA and 1% (w/w) calcium bentonite clay (without soaking in  $\text{CaCl}_2$ ) compared to those with 2% calcium bentonite clay,  $t$  statistic and  $t$  critical were found to be 2.6 and 4.3, respectively. While differences

**Fig. 1** Sorption capacity of Cu(II) at equilibrium (after 24 h of soaking), for different sorbents. Clay is calcium bentonite clay, and Ca indicates that sorbents were crosslinked with  $\text{CaCl}_2$

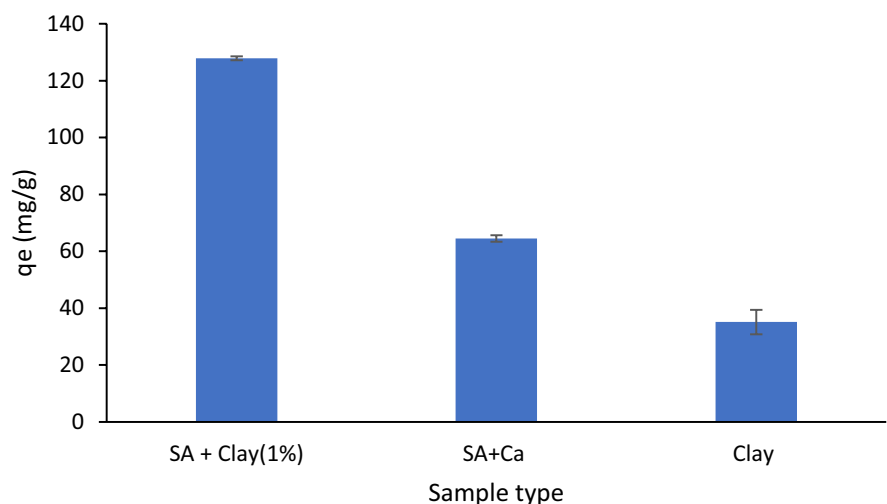
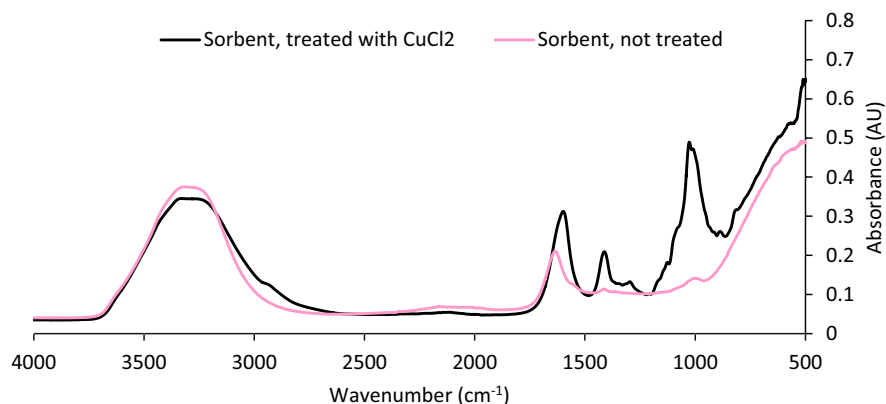


**Fig. 2** ATR-FTIR spectrum of sorbents obtained with SA and 1% (w/w) calcium bentonite clay (without soaking in  $\text{CaCl}_2$ ), following 24 h sorption of copper ions from a solution containing 0.1 M  $\text{CuCl}_2$



between the sorption capacity of SA + clay (1%) and SA + clay (2%) were statistically significant (based on a *t*-test), differences between samples prepared with  $\text{Ca}^{2+}$  (such as SA + Clay 1% + Ca, SA + Clay 2% + Ca, SA + Ca) and of clay alone were not statistically significant. In the case of sorbents obtained with SA and 1% (w/w) calcium bentonite clay (without soaking in  $\text{CaCl}_2$ ) compared to those without 1% calcium bentonite clay, *t* statistic and *t* critical were found to be 2.1 and 4.3 respectively.

This is likely because calcium bentonite clay alone had fewer binding sites compared to SA, although its addition to SA-based sorbents was beneficial to strengthen the material. This hypothesis is supported by the fact that calcium bentonite clay alone had lower sorption capacity compared to composite SA-clay sorbents (obtained without soaking in  $\text{CaCl}_2$ ).

Crosslinking with  $\text{CaCl}_2$  also decreased sorption capacity.  $\text{CaCl}_2$  has the potential strengthen sorbents because calcium ions crosslink SA (Lamont et al., 2020). However,  $\text{CaCl}_2$ -crosslinked sorbents containing calcium bentonite clay performed significantly worse than their counterparts not crosslinked with  $\text{CaCl}_2$ . Specifically, when sorbents were crosslinked using  $\text{CaCl}_2$ , their sorption capacity was  $q_e = 73.1 \pm 1.5$  mg/g and  $q_e = 77.1 \pm 0.7$  mg/g for sorbents containing 1% w/w and 2% w/w bentonite, respectively. Also,  $\text{CaCO}_3$  crosslinked sorbents without calcium bentonite clay had the lowest sorption capacity, with  $q_e = 64.5 \pm 1.1$  mg/g. The low sorption capacity of SA-based sorbents crosslinked with either  $\text{CaCl}_2$  or  $\text{CaCO}_3$  is in agreement with a previous study (Telepanich et al., 2021). This is likely due to  $\text{Ca}^{2+}$  ions occupying sorption sites and crosslinking SA, thereby decreasing surface area (X.

Gao et al., 2020). In sorbents prepared without  $\text{CaCl}_2$  or  $\text{CaCO}_3$ , some of the binding sites would be occupied, because calcium bentonite clay would release  $\text{Ca}^{2+}$ . Nonetheless, the number of occupied binding sites increases following immersion in  $\text{CaCl}_2$  solution or with the replacement of calcium bentonite clay ( $(\text{Na,Ca})_{0.33}(\text{Al,Mg})_2(\text{Si}_4\text{O}_{10})(\text{OH})_2 \cdot n\text{H}_2\text{O}$ ) with  $\text{CaCO}_3$  (which has a significantly higher  $\text{Ca}^{2+}$  content compared to clay). These sorbents were not used for the following analyses, which include the dynamic study of copper removal from water, as well as the removal of zinc from water.

The sorption capacity ( $q_e = 127.9 \pm 0.6$  mg/g) determined in this study with SA-based sorbents containing 1% (w/w) calcium bentonite clay (without crosslinking  $\text{CaCl}_2$ ) was significantly higher than that of SA-based sorbents used in other studies. For example, the sorption capacity at equilibrium of magnetic bentonite, carboxymethyl chitosan, and sodium alginate composite hydrogel beads used for Cu(II) removal was  $q_e = 56.79$  mg/g (H. Zhang et al., 2019). Another study that used porous freeze-dried SA and calcium carbonate sorbents for Cu(II) removal reports  $q_e = 33.88$  mg/g for Cu(II) removal (Hu et al., 2020). Nonetheless, one study reports a higher  $q_e$  compared to the ones for our sorbents. Specifically, Zhan et al. used sorbents made with cellulose and sodium alginate chemically modified with polyethyleneimine, and report  $q_e = 177.1$  mg/g for Cu(II) removal (Zhan et al., 2018). While effective, these beads contained polyethyleneimine, which is toxic to cells at high concentrations (Vanča et al., 2004).

While sorbents proposed in this study have lower sorption capacity than some of the ones previously developed, their facile fabrication and their

completely non-toxic composition render them promising for water purification. Additionally, due to the gas produced during pore formation, these sorbents floated even after shaking in solutions for 24 h, suggesting that they could be easily collected if used for surface water purification. Future research should focus on further improving sorption capacity, while using completely natural materials for facile sorbent fabrication.

In summary, the most effective sorbent for Cu(II) was obtained with SA and 1% calcium bentonite clay, without crosslinking with CaCl<sub>2</sub>. Optical microscopy images of this sorbent can be seen in Fig. 3. Pores within the sorbent structure increase surface area and facilitate the movement of Cu(II) ions throughout the sorbent, thereby enhancing sorption. Pore size in the sorbents shrank after sorption of Cu(II), as the Cu(II) ions acted as a crosslinker for SA. Crosslinking of SA by Cu(II) can occur through partially ionic or coordinate bonds (Treenate & Monvisade, 2017).

### 3.2 Effect of Adsorbent Composition on Zn(II) Sorption at Equilibrium

Similar to the sorption of Cu(II), SA-based sorbents containing calcium bentonite clay (1% w/w) had the highest sorption capacity at equilibrium, with  $q_e = 148.1 \pm 0.2$  mg/g (Fig. 4). Sorption of zinc ions onto this sorbent was also confirmed by ATR-FTIR, which showed changes in the ATR-FTIR sorbents following a 24-h period as seen in Fig. 5.

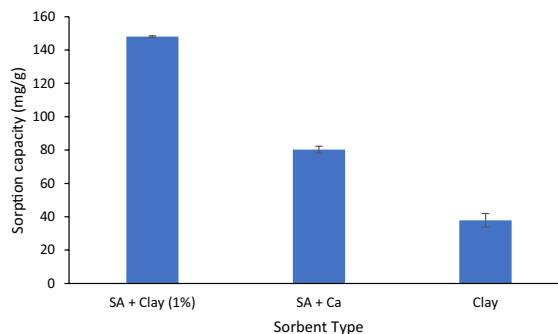


**Fig. 4** Sorption capacity at equilibrium (after 24 h of soaking) for SA sorbents used for the sorption of 0.1 M Zn(II)Cl<sub>2</sub> solutions. Clay is calcium bentonite clay, and Ca indicates that sorbents were crosslinked with CaCl<sub>2</sub>. Differences between the sorption capacity of SA-based sorbents prepared with calcium and without clay (SA + Ca) and of clay alone were not statistically significant. Differences between these samples and SA + clay (1%) were statistically significant (based on a *t*-test, as discussed in the text)

As with ATR-FTIR spectra for alginate-based sorbents before and after sorption of Cu<sup>2+</sup> ions, stretching vibrations of -OH at  $\approx 3000$  cm<sup>-1</sup> can be seen before and after Zn<sup>2+</sup> sorption. Additionally, the peak at  $\approx 1600$  cm<sup>-1</sup> is representative of the stretching of COO<sup>-</sup> bonds and bending vibration of C-C is represented by the absorbance peak at  $\approx 1400$  cm<sup>-1</sup>. These absorbance peaks were detected in a previous study (Mikula et al. 2019). The change in the shape of the spectrum in the fingerprint region following zinc sorption indicates that functional groups in the

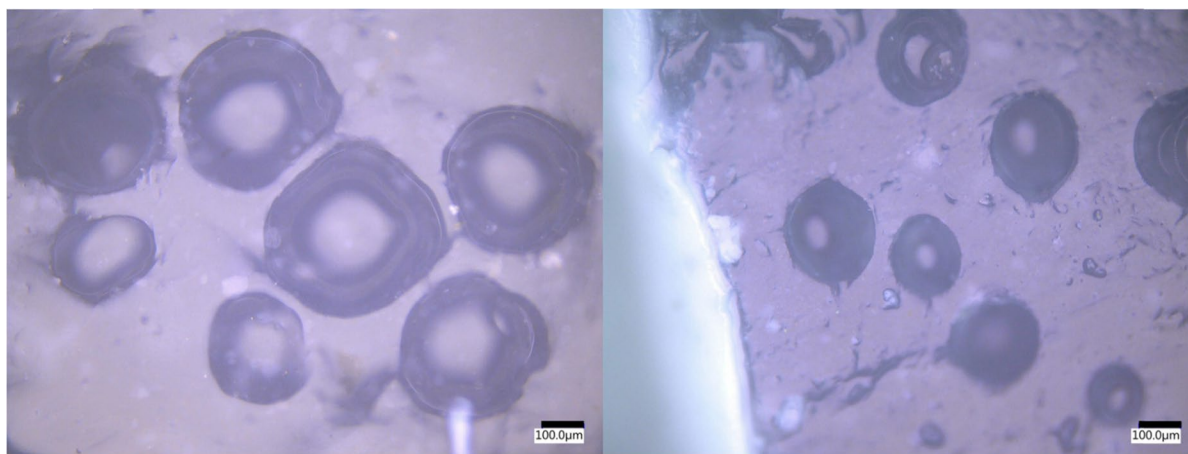
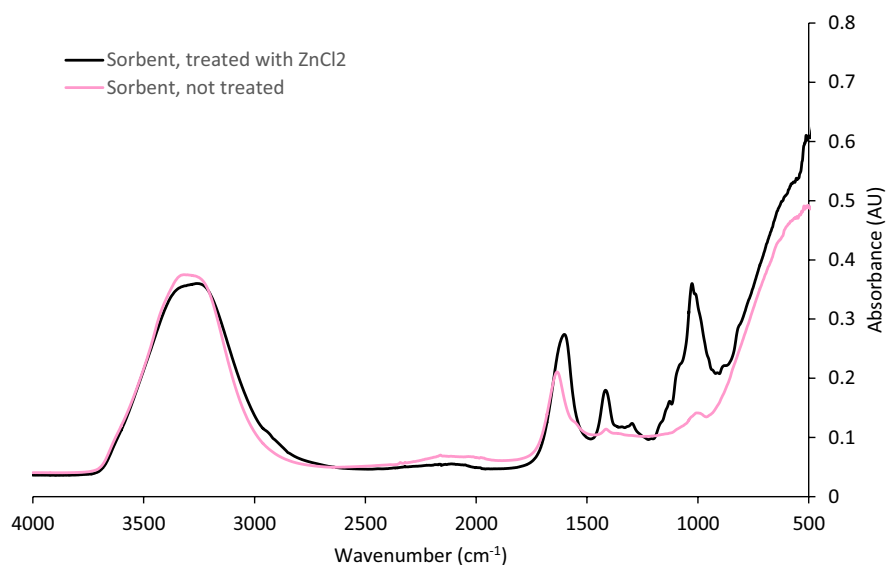


**Fig. 3** Optical microscopy of SA and calcium bentonite clay (1% w/w) sorbent before (left) and after soaking in 0.1 M CuCl<sub>2</sub> solution for 24 h. The scale bar is 100 μm



**Fig. 5** ATR-FTIR spectrum of sorbents obtained with SA and 1% (w/w) calcium bentonite clay (without soaking in  $\text{CaCl}_2$ ), following 24 h sorption of zinc ions from a solution containing 0.1 M  $\text{ZnCl}_2$



alginate-based sorbent were involved in ion binding (Mikula et al. 2019).

Sorbents containing no calcium bentonite clay had lower sorption capacity (with  $q_e = 80.3 \pm 0.3$  mg/g), while bentonite clay alone had a sorption capacity  $q_e = 37.9 \pm 0.2$  mg/g. The  $P$ -value of this data set was found to be  $1.99 \times 10^{-4}$ , suggesting that it is statistically significant. Note that SA-based sorbents containing 1% calcium bentonite clay had a higher sorption capacity  $q_e$  than the sum of the  $q_e$  of the individual components (SA and calcium bentonite clay). This suggests that the two components act synergistically in enabling  $\text{Zn(II)}$  sorption. As observed for  $\text{Cu(II)}$ , sorption of  $\text{Zn(II)}$  decreased when sorbents were crosslinked with  $\text{CaCl}_2$ . As highlighted in Sect. 3.1, calcium ions could occupy binding sites, thereby decreasing sorption.

Note that the pH of a 0.1-M  $\text{ZnCl}_2$  solution is 4.4, while the pH of a 0.1-M  $\text{CuCl}_2$  solution is 3. This difference in hydronium ion concentration could be the reason the sorption capacity at equilibrium was higher for zinc ions ( $127.9 \pm 0.6$  mg/g and  $148.1 \pm 0.2$  mg/g for  $\text{Cu(II)}$  and  $\text{Zn(II)}$ , respectively). This is because positively charged ions may be able to compete with the desired metals for binding sites in the sorbent. In this study, the pH was not adjusted as in preliminary trials it was found that the salts produced the insoluble metal hydroxide when base was added.

In this study, the sorption capacity for  $\text{Zn(II)}$  was found to be relatively high when compared to some

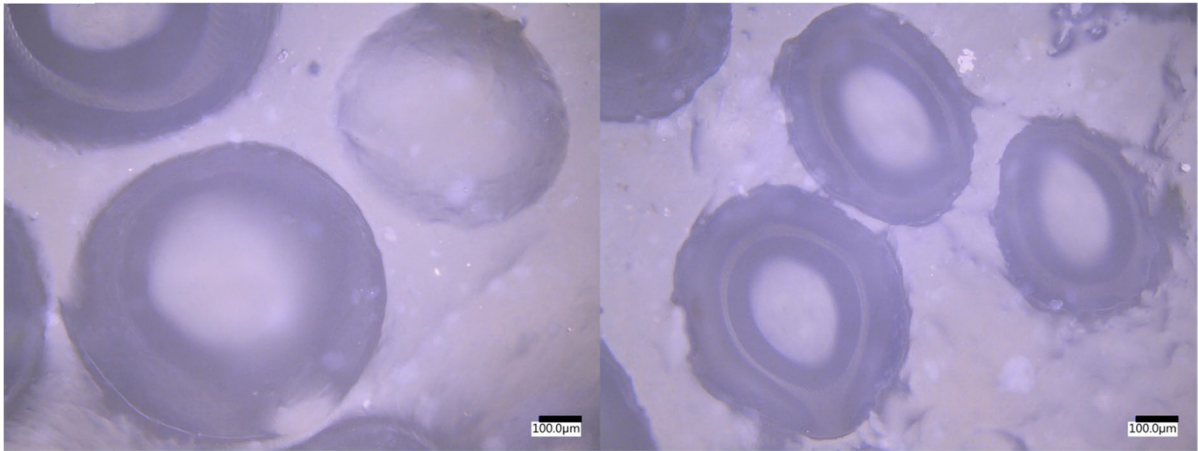
other studies. For example, a composite of combusted coal gangue with SA had a sorption capacity of  $q_e = 77.68$  mg/g for  $\text{Zn(II)}$  (Mohammadi et al., 2019). Additionally, sorbents made with cellulose and SA chemically modified with polyethyleneimine had a maximum sorption capacity of  $q_e = 110.2$  mg/g for  $\text{Zn(II)}$  (Zhan et al., 2018). Due to the high sorption capacity and simplicity of production, our sorbents would be advantageous for the removal of  $\text{Zn(II)}$  from contaminated water.

Figure 6 shows optical microscopy images of SA-based sorbents containing 1% (w/w) calcium bentonite clay. Similar to observations with  $\text{Cu(II)}$ , pore size in the sorbents shrank after sorption of  $\text{Zn(II)}$ . Similar to  $\text{Cu(II)}$ ,  $\text{Zn(II)}$  can crosslink SA through partially ionic or coordinate bonds (Treenate & Monvisade, 2017).

### 3.3 Sorption Kinetics

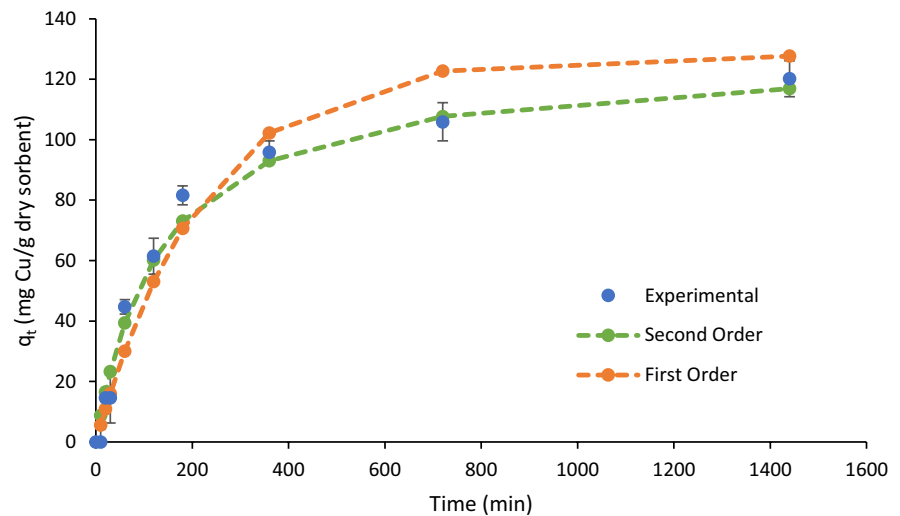
The most efficient SA-based sorbent was prepared with SA and 1% (w/w) bentonite clay, without crosslinking with  $\text{CaCl}_2$ , as discussed in Sects. 3.1 and 3.2. This sorbent was therefore used to investigate the sorption kinetics described in this section.

Figure 7 shows the sorption kinetics of  $\text{Cu(II)}$  onto SA-based sorbents containing 1% calcium bentonite clay. The rate constants  $k_1$  (for the pseudo first order model) and  $k_2$  (for the pseudo second-order model) were found to be  $4.47 \times 10^{-3}$  and  $5.80 \times 10^{-5}$ ,



**Fig. 6** Optical microscopy of SA and clay (1% w/w) sorbent before (left) and after soaking in 0.1 M ZnCl<sub>2</sub> solution for 24 h. The scale bar is 100 μm

**Fig. 7** Sorption kinetics of Cu(II) onto SA-based sorbents containing 1% calcium bentonite clay



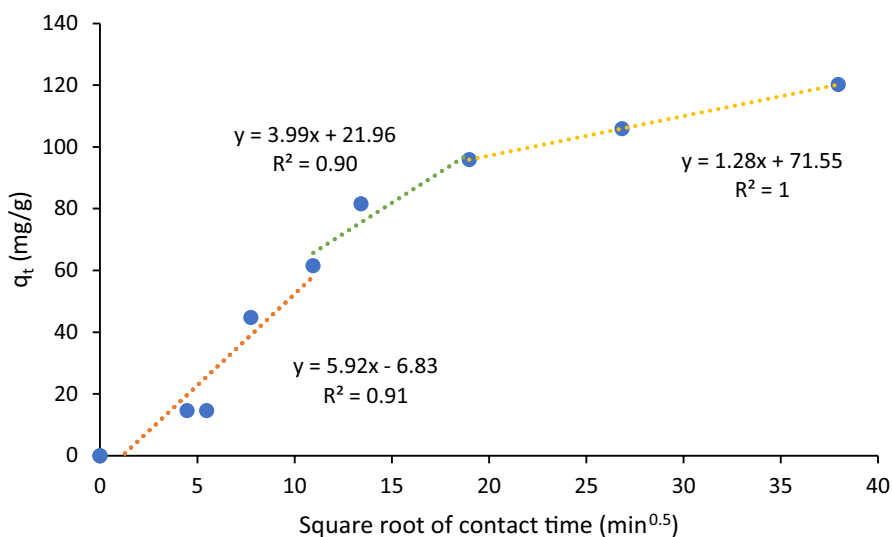
respectively. The data were best described by pseudo second-order kinetics, whereas first-order kinetic models were less suited to describe them (as seen from the poor fit to the data, Fig. 7).

The pseudo second-order model accounts for sorption capacity, rather than concentration of the sorbates (in this case (Cu(II) ions) (Simonin, 2016). This model takes into account external liquid membrane diffusion, internal particle diffusion, and surface adsorption (Sahoo & Prelot, 2020). It is based on the assumption that the rate limiting step is the chemical process of sorption (chemisorption) (Ncibi et al., 2008). The fact that the second-order kinetic model is best suited to represent our data indicates that the rate

limiting step is chemisorption of Cu(II) ions onto the sorbent, rather than the rate of their diffusion into it.

Intraparticle diffusion of Cu(II) into the sorbents can be seen in Fig. 8. Previous studies have shown that the plot of  $q_t$  vs  $t^{0.5}$  can be multi-linear, suggesting that several steps occur during the sorption process (Ncibi et al., 2008; Sun & Yang, 2003). It is clear that the sorption rate ( $k_i$ ) was highest in the first stage ( $k_{i1}=5.92$ ), followed by the second stage ( $k_{i2}=3.99$ ), and it was lowest in the third stage ( $k_{i3}=1.28$ ). The first and fastest stage corresponds to external surface (or instantaneous) adsorption (Sun & Yang, 2003; F. C. Wu et al., 2001). The second stage corresponds to gradual sorption, where intraparticle diffusion is

**Fig. 8** Intraparticle diffusion plot of  $q_t$  vs  $t^{0.5}$  for Cu(II). The filled circular symbols correspond to experimental data. The dashed lines represent the lines of best fit for sub-sets of experimental data



rate controlled as the solute diffuses into the pores of the sorbent towards the interior (Sun & Yang, 2003; F. C. Wu et al., 2001). Finally, the third stage corresponds to equilibrium, where sorption of the solute on the interior surfaces of the sorbent occurs, and diffusion begins to slow down (Sun & Yang, 2003; F. C. Wu et al., 2001). The decrease in slope from the first to third stages suggests that the sorption process

begins with surface adsorption, and is followed by the rate-controlled step of intraparticle diffusion.

Cu(II) penetration into the sorbents over time is clearly demonstrated by the blue discoloration of the cross-sections of the sorbents, as shown in Fig. 9. It is evident that the sorbent is fully penetrated at 3 h. This is consistent with the sorption kinetics shown in Fig. 7, as the sorption capacity starts to plateau at approximately 3 h. Visually, it is clear that samples

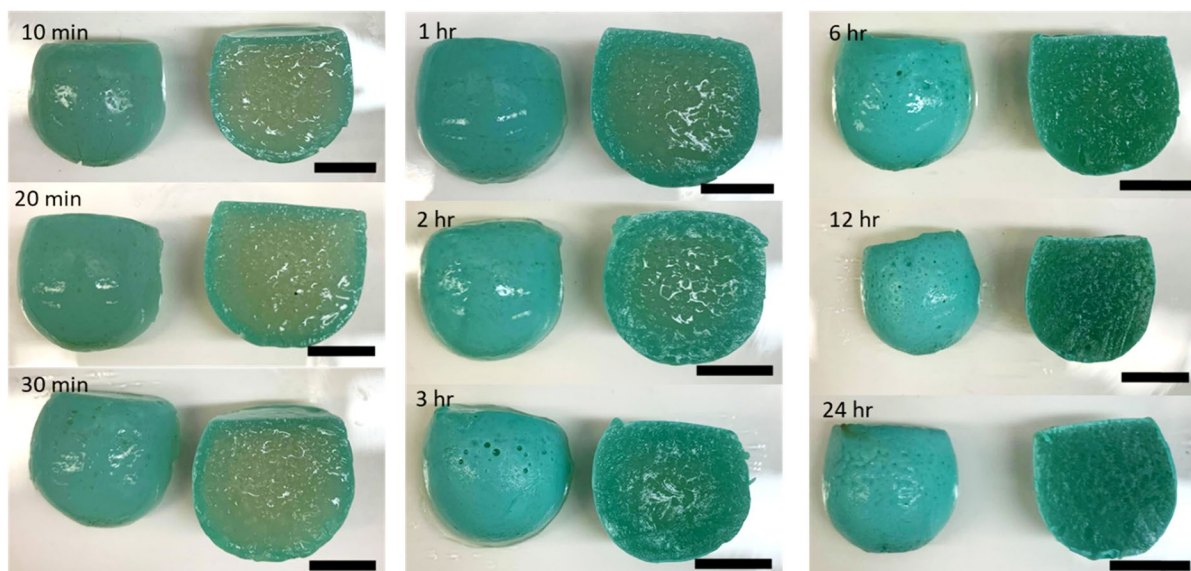


**Fig. 9** Cross-sections of SA-based sorbents containing 1% calcium bentonite clay after various sorption times of Cu(II). Scale is shown in the bottom right corner and is equal to 1 cm

left in solution for 6, 12, and 24 h have similar color, in agreement with the fact that  $q_t$  remained largely similar after 3 h (Fig. 7).

The sorption kinetics of Zn(II) are shown in Fig. 10. In the case of Zn(II), the rate constants  $k_1$  (for the pseudo first-order model) and  $k_2$  (for the pseudo second order model) were found to be  $9.71 \times 10^{-3}$  and  $3.29 \times 10^{-5}$ , respectively. Dissimilar to Cu(II), the data are best described by pseudo first-order kinetics (as evident from the poor fit of the second-order model to the data; Fig. 10). The pseudo first-order model only takes into account the relationship between concentration of the sorbate (Zn(II) in this

case) and sorption rate (Simonin, 2016). It is common for kinetic observations to follow this model when sorption occurs by way of diffusion through the interface (Sahoo & Prelot, 2020). This indicates that the rate limiting step of Zn(II) sorption is its diffusion into the sorbent, rather than its chemisorption onto it.

Intraparticle diffusion of Zn(II) into our sorbents is given in Fig. 11. Similar to the observations for Cu(II), the sorption rate ( $k_i$ ) for Zn(II) was highest in the first stage ( $k_{i1}=7.35$ ) followed by the second stage ( $k_{i2}=4.82$ ). This trend suggests that the sorption process of Zn(II) onto SA-based sorbents with 1% calcium bentonite clay starts with surface sorption

**Fig. 10** Sorption kinetics of Zn(II) onto SA-based sorbents containing 1% calcium bentonite clay

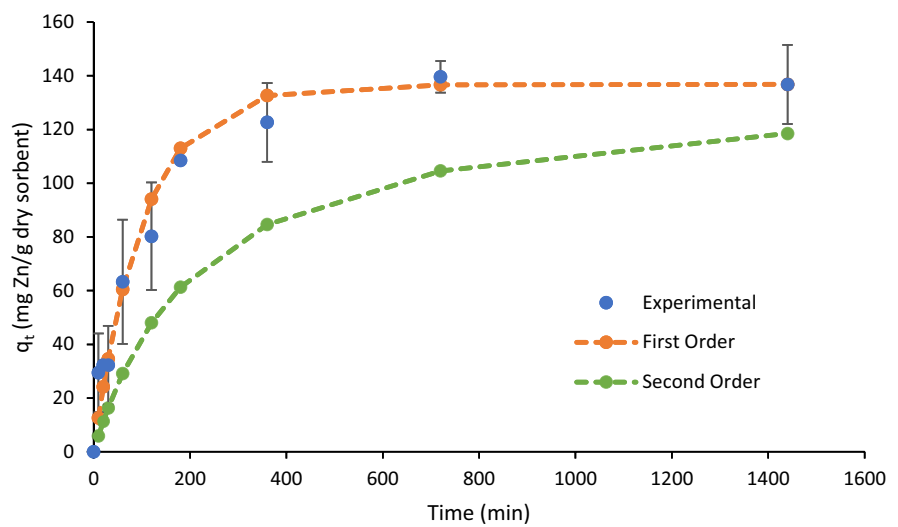
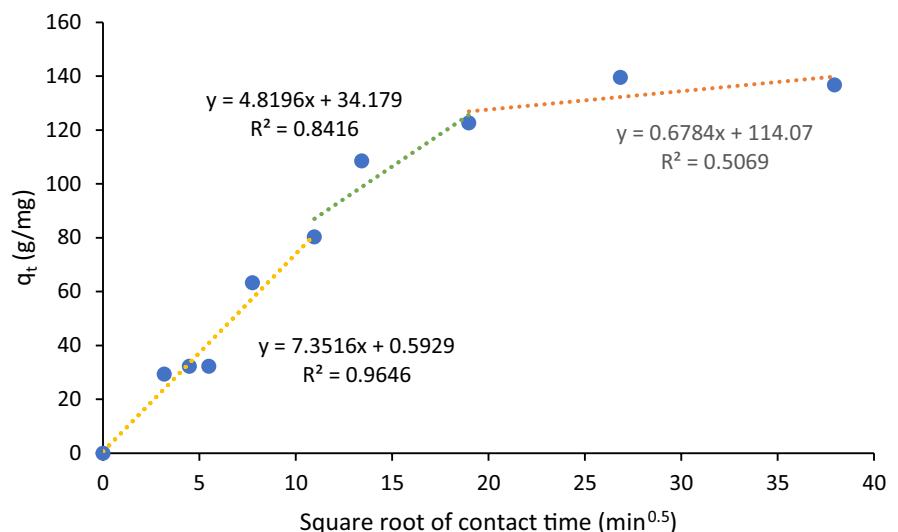


**Fig. 11** Intraparticle diffusion plot of  $q_t$  vs  $t^{0.5}$  for Zn(II). The filled circular symbols correspond to experimental data. The dashed lines represent the lines of best fit for sub-sets of experimental data



followed by the rate controlled step of intraparticle diffusion. Despite this similarity, the sorption process of Zn(II) and Cu(II) followed different order models, as previously highlighted, and the relative rate of each sorption stage of intraparticle diffusion also differed between the two ions. Specifically, the first and second stages of intraparticle diffusion were faster for Zn(II) than for Cu(II). This result indicates that while our sorbents are effective for both Cu(II) and Zn(II) removal, sorbent optimization may require different changes for each of these two contaminants.

### 3.4 Applicability of Alginate-Based Sorbents for the Removal of Other Metal Ions

Additional trials using sorbents obtained with SA and 1% (w/w) calcium bentonite clay on FeCl<sub>3</sub> and NiCl<sub>2</sub> were performed in the same manner as those done with ZnCl<sub>2</sub> and CuCl<sub>2</sub>. It was found that the  $q_e$  (after 24 h of soaking in 0.1 M solutions) for sorption of FeCl<sub>3</sub> and NiCl<sub>2</sub> was  $83 \pm 7$  mg/g and  $149.3 \pm 14$  mg/g, respectively. Recall that the  $q_e$  was  $127.9 \pm 0.6$  mg/g and  $148.1 \pm 0.2$  mg/g for Cu(II) and Zn(II), respectively. Divalent NiCl<sub>2</sub> had a comparable  $q_e$  to that seen with ZnCl<sub>2</sub> and CuCl<sub>2</sub>, while the  $q_e$  of FeCl<sub>3</sub> was significantly lower. It can be seen that alginate-based sorbents are more selective towards divalent ions, as reported in previous studies (Paudyal et al., 2013). Future research should focus on a wider variety of ions.

## 4 Conclusions

Overall, the sorption of Cu(II) and Zn(II) by SA-based sorbents was enhanced by the addition of calcium bentonite clay at 1% w/w concentrations. Controlling the porosity of SA-based sorbents by an acid base reaction also enhanced sorption. The maximum sorption capacity at equilibrium of SA-based sorbents was  $127.9 \pm 0.6$  mg/g and  $148.1 \pm 0.2$  mg/g for Cu(II) and Zn(II), respectively. Crosslinking with CaCl<sub>2</sub> decreased sorption capacity. Sorption kinetics were determined for SA-based sorbents containing 1% calcium bentonite clay. The sorption of Zn(II) with followed pseudo first-order kinetics (with a  $k_1 = 9.71 \times 10^{-3}$ ), indicating that the rate limiting step was the diffusion of ions into the sorbent (rather than chemisorption onto the sorbent). The sorption of

Cu(II) followed pseudo second-order kinetics (with a  $k_2 = 5.80 \times 10^{-5}$ ), suggesting that the rate limiting step was the chemisorption of Cu(II) onto the sorbents (rather than the rate of diffusion of ions into the sorbent). Optical microscopy images of the sorbent cross-section demonstrated that the sorbent pores shrank following sorption of either Zn(II) or Cu(II), due to crosslinking of alginate by these metal ions. Moreover, Cu(II) diffusion into the sorbents was indicated by the blue discoloration of their cross sections. The slope of the curves of  $q_t$  vs  $t^{0.5}$  (intraparticle diffusion plots) decreased from the first to third stages, indicating that the sorption process of both Zn(II) and Cu(II) starts with surface adsorption and is followed by the rate controlled step of intraparticle diffusion. Note that sorbents obtained with SA and 1% (w/w) calcium bentonite clay could also sorb Ni(II) and Fe(III), to a lesser extent. In particular, while divalent NiCl<sub>2</sub> had a comparable  $q_e$  to that seen with ZnCl<sub>2</sub> and CuCl<sub>2</sub>, the  $q_e$  of FeCl<sub>3</sub> was significantly lower. These results indicate that alginate-based sorbents are more selective towards divalent ions. These sorbents are promising options for the purification of water polluted by divalent ions, as they are simple to fabricate and have good sorption capacity. Future research should focus on further improving the sorption capacity of our natural sorbents, while maintaining their non-toxic composition and ease of fabrication.

**Funding** The authors received financial support from the Natural Sciences and Engineering Research Council of Canada (provided through an NSERC Discovery grant, awarded to Dr. Erica Pensini, RGPIN-2018-04636).

**Data Availability** The datasets generated during and/or analyzed during the current study are available from the corresponding author on reasonable request.

### Declarations

**Conflict of Interest** The authors declare no competing interests.

## References

- An, B., Lee, H., Lee, S., Lee, S.-H., & Choi, J.-W. (2015). Determining the selectivity of divalent metal cations for the carboxyl group of alginate hydrogel beads during competitive sorption. *Journal of Hazardous Materials*, 298, 11–18. <https://doi.org/10.1016/j.jhazmat.2015.05.005>

- Anirudhan, T. S., Jalajamony, S., & Sreekumari, S. S. (2012). Adsorption of heavy metal ions from aqueous solutions by amine and carboxylate functionalised bentonites. *Applied Clay Science*, 65–66, 67–71. <https://doi.org/10.1016/j.clay.2012.06.005>
- Ates, B., Koytepe, S., Ulu, A., Gurses, C., & Thakur, V. K. (2020). Chemistry, structures, and advanced applications of nanocomposites from biorenewable resources. *Chemical Reviews*, 120(17), 9304–9362. <https://doi.org/10.1021/acs.chemrev.9b00553>
- Batmaz, R., Mohammed, N., Zaman, M., Minhas, G., Berry, R. M., & Tam, K. C. (2014). Cellulose nanocrystals as promising adsorbents for the removal of cationic dyes. *Cellulose*, 21(3), 1655–1665. <https://doi.org/10.1007/s10570-014-0168-8>
- Bertagnolli, C., Uhart, A., Dupin, J.-C., da Silva, M. G. C., Guibal, E., & Desbrieres, J. (2014). Biosorption of chromium by alginate extraction products from *Sargassum filipendula*: Investigation of adsorption mechanisms using X-ray photoelectron spectroscopy analysis. *Bioresource Technology*, 164, 264–269. <https://doi.org/10.1016/j.biortech.2014.04.103>
- Borbély, G., & Nagy, E. (2009). Removal of zinc and nickel ions by complexation–membrane filtration process from industrial wastewater. *Desalination*, 240(1), 218–226. <https://doi.org/10.1016/j.desal.2007.11.073>
- Botelho Junior, A. B., Dreisinger, D. B., & Espinosa, D. C. R. (2019). A review of nickel, copper, and cobalt recovery by chelating ion exchange resins from mining processes and mining tailings. *Mining Metallurgy & Exploration*, 36(1, SI), 199.
- Burton, G. A., Nguyen, L. T. H., Janssen, C., Baudo, R., McWilliam, R., Bossuyt, B., et al. (2005). Field validation of sediment zinc toxicity. *Environmental Toxicology and Chemistry*, 24(3), 541. <https://doi.org/10.1897/04-031r.1>
- Choi, J.-W., Song, M.-H., Bediako, J. K., & Yun, Y.-S. (2020). Sequential recovery of gold and copper from bioleached wastewater using ion exchange resins. *Environmental Pollution*, 266, 115167. <https://doi.org/10.1016/j.envpol.2020.115167>
- Christidis, G. E., Blum, A. E., & Eberl, D. D. (2006). Influence of layer charge and charge distribution of smectites on the flow behaviour and swelling of bentonites. *Applied Clay Science*, 34(1), 125–138. <https://doi.org/10.1016/j.clay.2006.05.008>
- Cruz-Briano, S. A., Medellín-Castillo, N. A., Torres-Dosal, A., Leyva-Ramos, R., Moreno-Piraján, J. C., Giraldo-Gutiérrez, L., et al. (2021). Bone char from an invasive aquatic specie as a green adsorbent for fluoride removal in drinking water. *Water, Air, & Soil Pollution*, 232(9), 346. <https://doi.org/10.1007/s11270-021-05286-x>
- Dahlan, I., Hafiz, M. (2011). Waste-derived siliceous materials as a novel sorbent for removal of Ni<sup>2+</sup> from aqueous solutions. *Water, Air, & Soil Pollution*, 223. <https://doi.org/10.1007/s11270-011-1042-z>
- de Moura, M. R., Guilherme, M. R., Campese, G. M., Radovanovic, E., Rubira, A. F., & Muniz, E. C. (2005). Porous alginate-Ca<sup>2+</sup> hydrogels interpenetrated with PNIPAAm networks: Interrelationship between compressive stress and pore morphology. *European Polymer Journal*, 41(12), 2845–2852. <https://doi.org/10.1016/j.eurpolymj.2005.06.007>
- Dechojarassri, D., Omote, S., Nishida, K., Omura, T., Yamaguchi, H., Furuike, T., & Tamura, H. (2018). Preparation of alginate fibers coagulated by calcium chloride or sulfuric acid: Application to the adsorption of Sr<sup>2+</sup>. *Journal of Hazardous Materials*, 355, 154–161. <https://doi.org/10.1016/j.jhazmat.2018.05.027>
- Dos Santos, V. C. G., De Souza, J. V. T. M., Tarley, C. R. T., Caetano, J., & Dragunski, D. C. (2011). Copper ions adsorption from aqueous medium using the biosorbent sugarcane bagasse in natura and chemically modified. *Water, Air, & Soil Pollution*, 216(1), 351–359. <https://doi.org/10.1007/s11270-010-0537-3>
- Fiset, J.-F., Blais, J.-F., Riveros, P. (2008). Review on the removal of metal ions from effluents using seaweeds, alginate derivatives and other sorbents. *Revue des sciences de l'eau*, 21. <https://doi.org/10.7202/018776ar>
- Flemming, C. A., & Trevors, J. T. (1989). Copper toxicity and chemistry in the environment: A review. *Water, Air, and Soil Pollution*, 44(1–2), 143–158. <https://doi.org/10.1007/bf00228784>
- Foong, C. Y., Wirzal, M. D. H., & Bustam, M. A. (2020). A review on nanofibers membrane with amino-based ionic liquid for heavy metal removal. *Journal of Molecular Liquids*, 297, 111793. <https://doi.org/10.1016/j.molliq.2019.111793>
- Gao, P., Li, K., Liu, Z., Liu, B., Ma, C., Xue, G., Zhou, M. (2014). Feather keratin deposits as biosorbent for the removal of methylene blue from aqueous solution: Equilibrium, kinetics, and thermodynamics studies. *Water Air and Soil Pollution*, 225. <https://doi.org/10.1007/s11270-014-1946-5>
- Gao, X., Guo, C., Hao, J., Zhao, Z., Long, H., & Li, M. (2020). Adsorption of heavy metal ions by sodium alginate based adsorbent—A review and new perspectives. *International Journal of Biological Macromolecules*, 164, 4423–4434. <https://doi.org/10.1016/j.ijbiomac.2020.09.046>
- Gao, X., Li, M., Zhao, Y., & Zhang, Y. (2019). Mechanistic study of selective adsorption of Hg<sup>2+</sup> ion by porous alginate beads. *The Chemical Engineering Journal*, 378, 122096. <https://doi.org/10.1016/j.ccej.2019.122096>
- Ghimire, K. N., Inoue, K., Ohto, K., & Hayashida, T. (2008). Adsorption study of metal ions onto crosslinked seaweed *Laminaria japonica*. *Bioresource Technology*, 99(1), 32–37. <https://doi.org/10.1016/j.biortech.2006.11.057>
- Homayouni, A., Ehsani, M., Azizi, A., Yarmand, M. S., & Razavi, S. (2007). Effect of lecithin and calcium chloride solution on the Microencapsulation process yield of calcium alginate beads. *Iranian Polymer Journal*, 16, 597–606.
- Hosseini, S. M., Alibakhshi, H., Jashni, E., Parviziyan, F., Shen, J. N., Taheri, M., et al. (2020). A novel layer-by-layer heterogeneous cation exchange membrane for heavy metal ions removal from water. *Journal of Hazardous Materials*, 381, 120884. <https://doi.org/10.1016/j.jhazmat.2019.120884>
- Hosterman, J. W., & Patterson, S. H. (1992). Bentonite and fuller's earth resources of the United States. *Professional Paper*. <https://doi.org/10.3133/pp1522>

- Hu, X., Long, L., Gong, T., Zhang, J., Yan, J., & Xue, Y. (2020). Enhanced alginate-based microsphere with the pore-forming agent for efficient removal of Cu(II). *Chemosphere*, 240, 124860. <https://doi.org/10.1016/j.chemosphere.2019.124860>
- Huo, H., Su, H., & Tan, T. (2009). Adsorption of Ag<sup>+</sup> by a surface molecular-imprinted biosorbent. *Chemical Engineering Journal - CHEM ENG J*, 150, 139–144. <https://doi.org/10.1016/j.cej.2008.12.014>
- Iyer, A., Pensini, E., Singh, A. (2019). Removal of hexavalent chromium from water using hydrochar obtained with different types of feedstock. *Canadian Journal of Civil Engineering*, 47. <https://doi.org/10.1139/cjce-2019-0215>
- Joseph, L., Jun, B.-M., Flora, J. R. V., Park, C. M., & Yoon, Y. (2019). Removal of heavy metals from water sources in the developing world using low-cost materials: A review. *Chemosphere*, 229, 142–159. <https://doi.org/10.1016/j.chemosphere.2019.04.198>
- Karatutlu, A., Barhoum, A., Sapelkin, A. (2018). Chapter 1 — Liquid-phase synthesis of nanoparticles and nanostructured materials. In A. Barhoum & A. S. H. Makhlof (Eds.), *Emerging applications of nanoparticles and architecture nanostructures* (1–28). Elsevier. <https://doi.org/10.1016/B978-0-323-51254-1.00001-4>
- Kayranli, B., Gok, O., Yilmaz, T., Gok, G., Celebi, H., Seckin, I. Y., & Kalat, D. (2021). Zinc removal mechanisms with recycled lignocellulose: From fruit residual to biosorbent then soil conditioner. *Water, Air, & Soil Pollution*, 232(8), 311. <https://doi.org/10.1007/s11270-021-05260-7>
- Khalil, H. P. S. A., Tye, Y. Y., Saurabh, C. K., Leh, C. P., Lai, T. K., Chong, E. W. N., et al. (2017). Biodegradable polymer films from seaweed polysaccharides: A review on cellulose as a reinforcement material. *eXPRESS Polymer Letters*, 11(4), 244–265. <https://doi.org/10.3144/expresspolymlett.2017.26>
- Krstić, V., Urošević, T., & Pešovski, B. (2018). A review on adsorbents for treatment of water and wastewaters containing copper ions. *Chemical Engineering Science*, 192, 273–287. <https://doi.org/10.1016/j.ces.2018.07.022>
- Lagaly, G. (1994). Bentonites: adsorbents of toxic substances. In M. J. Schwuger, F. H. Haegel (Eds.), *Surfactants and colloids in the environment* (61–72). Darmstadt: Steinkopff. <https://doi.org/10.1007/BFb0115705>
- Lamont, K., Marangoni, A. G., & Pensini, E. (2020). “Emulsion locks” for the containment of hydrocarbons during surfactant flushing. *Journal of Environmental Sciences*, 90, 98–109. <https://doi.org/10.1016/J.JES.2019.11.021>
- Lee, K. Y., & Mooney, D. J. (2012). Alginate: Properties and biomedical applications. *Progress in Polymer Science*, 37(1), 106–126. <https://doi.org/10.1016/j.progpolymsci.2011.06.003>
- Liu, Y., Hu, X., Wang, H., Chen, A., Liu, S., Guo, Y., et al. (2013). Photoreduction of Cr(VI) from acidic aqueous solution using TiO<sub>2</sub>-impregnated glutaraldehyde-crosslinked alginate beads and the effects of Fe(III) ions. <https://doi.org/10.1016/J.CEJ.2013.04.048>
- Maguire, T. J., Wellen, C., Stammmer, K. L., & Mundle, S. O. C. (2018). Increased nutrient concentrations in Lake Erie tributaries influenced by greenhouse agriculture. *Science of the Total Environment*, 633, 433–440. <https://doi.org/10.1016/j.scitotenv.2018.03.188>
- Malicevic, S., Pacheco, A. P. G., Lamont, K., Estepa, K. M., Daguppati, P., van de Vegte, J., et al. (2020). Phosphate removal from water using alginate/carboxymethylcellulose/aluminum beads and plaster of paris. *Water Environment Research*, 92(9), 1255–1267. <https://doi.org/10.1002/wer.1321>
- Menzel, K., Barros, L., García, A., Ruby-Figueroa, R., & Estay, H. (2021). Metal sulfide precipitation coupled with membrane filtration process for recovering copper from acid mine drainage. *Separation and Purification Technology*, 270, 118721. <https://doi.org/10.1016/j.seppur.2021.118721>
- Mikula, K., Skrzypczak, D., Ligas, B. and Witek-Krowiak, A., (2019). Preparation of hydrogel composites using Ca<sup>2+</sup> and Cu<sup>2+</sup> ions as crosslinking agents. *SN Applied Sciences*, 1(6), 1–15.
- Miller, D. G. (1979). Colorimetric Determination of zinc with zincon and cyclohexanone. *Journal (water Pollution Control Federation)*, 51(10), 2402–2412.
- Mohammadi, R., Azadmehr, A., & Maghsoudi, A. (2019). Fabrication of the alginate-combusted coal gangue composite for simultaneous and effective adsorption of Zn(II) and Mn(II). *Journal of Environmental Chemical Engineering*, 7(6), 103494. <https://doi.org/10.1016/j.jece.2019.103494>
- Mourpichai, A., Jintakosol, T., & Nitayaphat, W. (2018). Adsorption of gold ion from a solution using montmorillonite/alginate composite. *Materials Today: Proceedings*, 5(7, Part 1), 14786–14792.
- Murray, A., & Örmeci, B. (2019). Use of polymeric sub-micron ion-exchange resins for removal of lead, copper, zinc, and nickel from natural waters. *Journal of Environmental Sciences*, 75, 247–254. <https://doi.org/10.1016/j.jes.2018.03.035>
- Ncibi, M. C., Mahjoub, B., & Seffen, M. (2008). Investigation of the sorption mechanisms of metal-complexed dye onto Posidonia oceanica (L.) fibres through kinetic modelling analysis. *Bioresource Technology*, 99(13), 5582–5589. <https://doi.org/10.1016/j.biortech.2007.10.040>
- Nishimura, H., & Sato, S. (1972, May 16). Method of producing polyvinyl acetal porous articles and the shaped porous articles made therefrom. <https://patents.google.com/patent/US3663470A/en>. Accessed 19 August 2021
- Ortiz-Soto, R., Leal, D., Gutierrez, C., Aracena, A., Rojo, A., & Hansen, H. K. (2019). Electrokinetic remediation of manganese and zinc in copper mine tailings. *Journal of Hazardous Materials*, 365, 905–911. <https://doi.org/10.1016/j.jhazmat.2018.11.048>
- Osman, I., Seyfullah, K., & Burcu, C. (2005). The effect of PEG on the water absorption capacity and rate of superabsorbent copolymers based on acrylic acid. *International Journal of Polymeric Materials and Polymeric Biomaterials*, 54(11), 1001–1008. <https://doi.org/10.1080/0091403905117704>
- Paudyal, H., Pangeni, B., Inoue, K., Kawakita, H., Ohto, K., Ghimire, K. N., & Alam, S. (2013). Preparation of novel alginate based anion exchanger from Ulva japonica and its application for the removal of trace concentrations of fluoride from water. *Bioresource Technology*, 148, 221–227. <https://doi.org/10.1016/j.biortech.2013.08.116>

- Pensini, E., Laredo, T., Earnden, L., Marangoni, A. G., & Ghazani, S. M. (2021). A 'three in one' complexing agent enables copper desorption from polluted soil, its removal from groundwater and its detection. *Colloids and Surfaces a: Physicochemical and Engineering Aspects*, 624, 126840. <https://doi.org/10.1016/j.colsurfa.2021.126840>
- Ren, Z.-L., Shao, L., & Zhang, G. (2012). Adsorption of phosphate from aqueous solution using an iron–zirconium binary oxide sorbent. *Water, Air, & Soil Pollution*. <https://doi.org/10.1007/s11270-012-1186-5>
- Rezaee, M., Ghomesheh, P. K., & Hosseini, A. M. (2017). Electrokinetic remediation of zinc and copper contaminated soil: A simulation-based study. *Civil Engineering Journal*, 3(9), 690–700. <https://doi.org/10.21859/cej-03096>
- Safieh, P., Pensini, E., Marangoni, A., Lamont, K., Ghazani, S. M., Callaghan-Patrarachar, N., et al. (2019). Natural emulsion gels and lecithin-based sorbents: A potential treatment method for organic spills on surface waters. *Colloids and Surfaces a: Physicochemical and Engineering Aspects*, 574, 245–259. <https://doi.org/10.1016/j.colsurfa.2019.04.090>
- Sahoo, T. R., Prelot, B. (2020). Chapter 7 - Adsorption processes for the removal of contaminants from wastewater: the perspective role of nanomaterials and nanotechnology. In B. Bonelli, F. S. Freyria, I. Rossetti, & R. Sethi (Eds.), *Nanomaterials for the Detection and Removal of Wastewater Pollutants* (161–222). Elsevier. <https://doi.org/10.1016/B978-0-12-818489-9.00007-4>
- Simonin, J.-P. (2016). On the comparison of pseudo-first order and pseudo-second order rate laws in the modeling of adsorption kinetics. *Chemical Engineering Journal*, 300, 254–263. <https://doi.org/10.1016/j.cej.2016.04.079>
- Sun, Q., & Yang, L. (2003). The adsorption of basic dyes from aqueous solution on modified peat-resin particle. *Water Research*, 37(7), 1535–1544. [https://doi.org/10.1016/S0043-1354\(02\)00520-1](https://doi.org/10.1016/S0043-1354(02)00520-1)
- Tan, W. S., & Ting, A. S. Y. (2014). Alginate-immobilized bentonite clay: Adsorption efficacy and reusability for Cu(II) removal from aqueous solution. *Bioresource Technology*, 160, 115–118. <https://doi.org/10.1016/j.biortech.2013.12.056>
- Tanaka, H., Matsumura, M., & Veliky, I. A. (1984). Diffusion characteristics of substrates in Ca-alginate gel beads. *Biotechnology and Bioengineering*, 26(1), 53–58. <https://doi.org/10.1002/bit.260260111>
- Tavares, D., Lopes, C., Coelho, J., Sánchez, M., García, A., Duarte, A., et al. (2011). Removal of arsenic from aqueous solutions by sorption onto sewage sludge-based sorbent. *Water, Air, & Soil Pollution*, 223. <https://doi.org/10.1007/s11270-011-1025-0>
- Telepanich, A., Marshall, T., Gregori, S., Marangoni, A. G., & Pensini, E. (2021). Graphene-alginate fluids as unconventional electrodes for the electrokinetic remediation of Cr(VI). *Water, Air, & Soil Pollution*, 232(8), 334. <https://doi.org/10.1007/s11270-021-05278-x>
- Treenate, P., & Monvisade, P. (2017). In vitro drug release profiles of pH-sensitive hydroxyethylacryl chitosan/sodium alginate hydrogels using paracetamol as a soluble model drug. *International Journal of Biological Macromolecules*, 99, 71–78. <https://doi.org/10.1016/j.ijbiomac.2017.02.061>
- Vancha, A. R., Govindaraju, S., Parsa, K. V., Jasti, M., González-García, M., & Ballesteros, R. P. (2004). Use of polyethyleneimine polymer in cell culture as attachment factor and lipofection enhancer. *BMC Biotechnology*, 4(1), 23. <https://doi.org/10.1186/1472-6750-4-23>
- Wang, L. P., & Chen, Y. J. (2019). Sequential precipitation of iron, copper, and zinc from wastewater for metal recovery. *Journal of Environmental Engineering*, 145(1), 04018130. [https://doi.org/10.1061/\(ASCE\)EE.1943-7870.0001480](https://doi.org/10.1061/(ASCE)EE.1943-7870.0001480)
- Wang, S., Vincent, T., Faur, C., & Guibal, E. (2018). A comparison of Palladium sorption using polyethyleneimine impregnated alginate-based and Carrageenan-based algal beads. *Applied Sciences*, 8(2), 264. <https://doi.org/10.3390/app8020264>
- Wee, null, & Gombotz, null. (1998). Protein release from alginate matrices. *Advanced Drug Delivery Reviews*, 31(3), 267–285. [https://doi.org/10.1016/s0169-409x\(97\)00124-5](https://doi.org/10.1016/s0169-409x(97)00124-5)
- Wu, F. C., Tseng, R. L., & Juang, R. S. (2001). Kinetic modeling of liquid-phase adsorption of reactive dyes and metal ions on chitosan. *Water Research*, 35(3), 613–618. [https://doi.org/10.1016/s0043-1354\(00\)00307-9](https://doi.org/10.1016/s0043-1354(00)00307-9)
- Wu, H., Wang, W., Huang, Y., Han, G., Yang, S., Su, S., et al. (2019). Comprehensive evaluation on a prospective precipitation-flotation process for metal-ions removal from wastewater simulants. *Journal of Hazardous Materials*, 371, 592–602. <https://doi.org/10.1016/j.jhazmat.2019.03.048>
- Wu, X., Sun, X., Pan, M., & Liu, H. (2017). Sustained drug release from chitosan@alginate microspheres with porous core and closed outer surface pore structure. *Journal of Controlled Release*, 259, e40. <https://doi.org/10.1016/j.jconrel.2017.03.105>
- Zhan, W., Xu, C., Qian, G., Huang, G., Tang, X., & Lin, B. (2018). Adsorption of Cu( ii ), Zn( ii ), and Pb( ii ) from aqueous single and binary metal solutions by regenerated cellulose and sodium alginate chemically modified with polyethyleneimine. *RSC Advances*, 8(33), 18723–18733. <https://doi.org/10.1039/C8RA02055H>
- Zhang, H., Omer, A. M., Hu, Z., Yang, L.-Y., Ji, C., & Ouyang, X. (2019). Fabrication of magnetic bentonite/carboxymethyl chitosan/sodium alginate hydrogel beads for Cu (II) adsorption. *International Journal of Biological Macromolecules*, 135, 490–500. <https://doi.org/10.1016/j.ijbiomac.2019.05.185>
- Zhang, Q., Du, Q., Hua, M., Jiao, T., Gao, F., & Pan, B. (2013). Sorption enhancement of lead ions from water by surface charged polystyrene-supported nano-zirconium oxide composites. *Environmental Science & Technology*, 47(12), 6536–6544. <https://doi.org/10.1021/es400919t>

**Publisher's Note** Springer Nature remains neutral with regard to jurisdictional claims in published maps and institutional affiliations.